Comparison of Solid-State and Solution Photophysical Properties of a Platinum(II) Biphenyl Dicarbonyl Complex: A Multiple-State Emission Study

Greg Y. Zheng and D. Paul Rillema*

Department of Chemistry, Wichita State University, Wichita, Kansas 67260-0051

Received May 16, 1997

$Pt(bph)(CO)_2$, where bph is the biphenyl dianion, displays multiple emission by altering the temperature, solvent, or its state. Emission spectra and emission quantum yields are concentration and excitation wavelength dependent. In dilute 4:1 ethanol/methanol at room temperature, a structured emission at high energy (~500 nm) occurs, but in the solid state a nonstructured emission centered at (~750 nm) is found. Between these extremes, two other emissions located at ~540 and ~650 nm are observed. Emissions from high energy to low energy are attributed to the following: triplet emission centered on the bph ligand, emission from a dimer (exciplex), emission from an aggregate, and emission from "stacked" platinum(II) crystals.

Introduction

Multiple-state emission[1−8] has been reported for several mixed-ligand transition metal complexes of Rh(III), Ir(III), Re(I), Ru(II), and Cu(I), but in most cases energy transfer occurs efficiently among excited states and single-state emission is observed from the lowest energy emitting state. Multiple-state emission in mixed-ligand transition metals is of great interest from a theoretical point of view. Such studies can provide valuable information in understanding the photophysics of transition metal complexes, such as the origins of multiple-state emission, the strength of coupling between the emitting states, the efficiency of energy transfer between excited states, equilibria between excited states, strong or weak kinetic coupling, interligand interactions, etc.

There is another class of compounds that give rise to multiple emission, not in the classical sense from the same molecule but from aggregates in solution which form from monomers due to weak bonding interactions. This has been especially true for platinum(II) complexes which often give rise to products produced from the same monomer differing in color and emission properties.[9−12]

Earlier, we[13−18] and others[19,20] reported emission from $Pt(bph)X_2$ and Pt(bph)L, where bph is the biphenyl dianion, X = py and CH_3CN, and L = COD, ethylene diammine, and bis(diphenylphospino)methane. Structured emission in solution at room temperature was observed from these complexes with emission maxima located near 500 nm and attributed to a triplet state associated with the bph ligand. Emission from $Pt(bph)(CO)_2$, however, was more complex as noted in our earlier reports on the synthesis and properties of $Pt(bph)(CO)_2$.[16] Here we report a detailed study on its excited-state properties. On the basis of these and a comparison with Pt(bph)(dppm), the multiple state emissions observed were assigned to triplet ligand-centered bph emission, emission from a species formed by intraligand interactions between different complexes or by metal−metal interactions, emission from an aggregate, and emission from the cystalline solid state.

Experimental Section

Materials. The preparation, purification and characterization of $Pt(bph)(CO)_2$ and Pt(bph)(dppm) were reported.[13,16] Methylene chloride and methanol were optima grade and purchased from Fisher Scientific. 2-Methyltetrahydrofuran (2-MeTHF) was 99% purity and used as purchased from Aldrich Chemical Co. Absolute ethanol was purchased from McCormick Distilling Co. Solvents consisting of CH_2Cl_2, 4:1 (v/v) 2-MeTHF/CH_2Cl_2, 4:1 (v/v) C_2H_5OH/CH_3OH, and 1:1 (v/v) 2-MeTHF/CH_2Cl_2 were used.

Physical Measurements. UV−visible spectra were recorded with a double beam Olis Cary 14 spectrophotometer. Emission and excitation spectra were recorded with a Spex Fluorolog 212 spectro-

---

(1) DeAmond, M. K.; Carlin, C. M. *Coord. Chem. Rev.* **1981**, *36*, 325.

(2) Casadonte, D. J., Jr.; McMillin, D. R. *J. Am. Chem. Soc.* **1987**, *109*, 331.

(3) Baggott, J. E.; Gregory, G. K.; Pilling, M. J. *J. Chem. Soc., Faraday Trans. 2* **1983**, *79*, 159.

(4) Cocks, A. T.; Wright, R. D.; Seddon, K. R. *Chem. Phys. Lett.* **1982**, *85*, 369.

(5) Belser, P.; von Zelewsky, A.; Juris, A.; Barigelletti, F.; Balzani, V. *Chem. Phys. Lett.* **1984**, *104*, 100.

(6) Zuleta, J. A.; Burbeery, M. S.; Eisenberg, R. *Coord. Chem. Rev.* **1990**, *97*, 47.

(7) Zuleta, J. A.; Bevilacqua, J. M.; Rehm, J. M.; Eisenberg, R. *Inorg. Chem.* **1992**, *31*, 1332.

(8) Kunkely, H.; Vogler, A. *J. Am. Chem. Soc.* **1990**, *112*, 5625.

(9) (a) Bailey, J. A.; Hill, M. G.; Marsh, R. E.; Miskowski, V. M.; Schaefer, W. P.; Gray, H. B. *Inorg. Chem.* **1995**, *34*, 4591. (b) Bailey, J. A.; Gray, H. B. *Acta Crystallogr.* **1992**, *C48*, 1420. (c) Bailey, J. A.; Miskowski, V. M.; Gray, H. B. *Acta Crystallogr.* **1993**, *C49*, 793.

(10) Yip, H.-K.; Che, C.-M.; Zhow, Z.-Y.; Mak, T. C. *J. Chem. Soc., Chem. Commun.* **1992**, 1369.

(11) Ratilla, E. M. A.; Scott, B. K.; Moxness, M. S.; Kostic, N. M. *Inorg. Chem.* **1990**, *29*, 918.

(12) Jennette, K. W.; Gill, J. T.; Sadownick, J. A.; Lippard, S. J. *J. Am. Chem. Soc.* **1976**, *98*, 6159.

(13) Chen, Y.-H. Physical and Photophysical Studies of a Series of Platinum(II) Complexes M.S. Thesis, The University of North Carolina at Charlotte, 1995.

(14) Blanton, C. B.; Rillema, D. P. *Inorg. Chim. Acta* **1990**, *168*, 145.

(15) Blanton, C. B.; Murtaza, Z.; Shaver, R. J.; Rillema, D. P. *Inorg. Chem.* **1992**, *31*, 3230.

(16) Chen, Y.-H.; Merkert, J. W.; Murtaza, Z.; Woods, C.; Rillema, D. P. *Inorg. Chim. Acta* **1995**, *240*, 41.

(17) Chen, Y.-H.; Woods, C.; Perkovic, M. W.; Rillema, D. P. *J. Chem. Crystallogr.* **1996**, *26*, 527.

(18) Zheng, G. Y.; Rillema, D. P.; DePriest, J.; Woods, C. Unpublished observations.

(19) Cornioley-Deuschel, C.; von Zelewsky, A. *Inorg. Chem.* **1987**, *26*, 3354.

(20) Maestri, M.; Sandrini, D.; Balzani, V.; von Zelewsky, A.; Deuschel-Cornioley, C.; Jolliet, P. *Helv. Chim. Acta* **1988**, *71*, 1053.

S0020-1669(97)00594-6 CCC: $15.00

Table 1. Effects of Solvent and Temperature on Emission Quantum Yields and Lifetimes of Pt(bph)$(CO)_2$[a]

solvents	quantum yield (296 K)	$\tau_{296\ \mathrm{K}}$ (μs)	$\tau_{77\ \mathrm{K}}$ (μs)
CH_2Cl_2	0.028 (ex. 280) 0.084 (ex. 300) 0.036 (ex. 330) 0.032 (ex. 400)	3.6 ± 0.2 (514, 555, 590)	
4:1 (v/v) 2-MeTHF/CH_2Cl_2	0.0094 (ex. 330)	0.71 ± 0.06 (506, 544, 590)	18.3 ± 0.7 (500) 10.0 ± 0.6 (539) 9.4 ± 0.4 (576) 4.7 ± 0.1 (644)
4:1 (v/v) C_2H_5OH/CH_3OH	0.036 (ex. 330)	2.2 ± 0.1 (506, 544, 590)	13.7 ± 0.2 (500) 13.7 ± 1.0 (539) 11.3 ± 0.3 (576)
crystal		0.84 ± 0.06 (727)	0.99 ± 0.02 (792)

[a] Samples were excited at 355 nm.

fluorometer and corrected for instrument response. Spectra of Pt(bph)$(CO)_2$ were obtained in CH_2Cl_2, 4:1 (v/v) 2-MeTHF/CH_2Cl_2, and 4:1 (v/v) C_2H_5OH/CH_3OH. Samples in CH_2Cl_2 were degassed by bubbling with Ar for 30 min prior to measurement. Samples in solvents 4:1 (v/v) 2-MeTHF/CH_2Cl_2, and 4:1 (v/v) C_2H_5OH/CH_3OH were degassed by at least three freeze−pump−thaw cycles prior to measurement. Samples in the solvent 1:1 (v/v) 2-MeTHF/CH_2Cl_2 were degassed by either three freeze−pump−thaw cycles or by bubbling with CO for 30 min prior to measurement. Excitation and emission spectra of needle crystals, recrystallized from CH_2Cl_2, were also studied.

Emission quantum yields were measured at various excitation wavelengths for Pt(bph)$(CO)_2$ in different solvents at room temperature. Rhodamine-B base ($\phi_r = 0.71$)[21] was used as the standard, and eq 1

$$\phi_s = \phi_r \frac{A_r}{A_s} \frac{I_s}{I_r} \frac{I_r^0}{I_s^0} \qquad (1)$$

was used to calculate emission quantum yields. In eq 1, ϕ_s is the quantum yield of the sample, ϕ_r is the quantum yield of the reference, A_s and A_r are the absorbance of the sample and reference at the excitation wavelength, respectively, I_s and I_r are the integrated areas under the emission spectra of interest, and I_s^0 and I_r^0 are the intensities of the incident light for the sample and reference, respectively.

Emission lifetimes were measured by exciting the samples at either the second harmonic or third harmonic or using an Opotek optical parametric oscillator pumped by a frequency tripled Nd:YAG laser (Continuum Surlite, run at ≤ 1.5 mJ/10 ns pulse). Spectral regions were isolated using a Hamamatsu R955 PMT in a cooled housing (−15 °C, Amherst) coupled to an Acton SpectraPro 275 monochromator. Transients were recorded with a LeCroy 9359A digital oscilloscope (1 Gs/s). Oscilloscope control and data curve fitting were accomplished with a program developed in-house. Emission lifetimes at 77 K were measured for samples immersed in a dewar filled with liquid N_2.

Results

UV−Vis Absorption Spectra. The room-temperature absorption spectra for Pt(bph)$(CO)_2$ in CH_2Cl_2 and 4:1 (v/v) C_2H_5OH/CH_3OH are shown in Figure 1 and compared to Pt(bph)(dppm) in CH_2Cl_2. Similar features are observed in the 350−300 nm region and assigned to metal-to-ligand charge transfer (MLCT). The absorption behavior of Pt(bph)$(CO)_2$ in 4:1 (v/v) 2-MeTHF/CH_2Cl_2 (not shown) is similar, but the solvent window only extends to 310 nm. There are substantive differences in the 250−300 nm region where the intensity of the intraligand transition in CH_2Cl_2 located at 282 nm is approximately 10 times more intense than in 4:1 (v/v) C_2H_5OH/CH_3OH. In addition, the bands in this region are more clearly resolved in 4:1 (v/v) C_2H_5OH/CH_3OH than in CH_2Cl_2. The absorptions of the standard, Pt(bph)(dppm) in this case, are less well resolved; the MLCT transition is red-shifted from 333 nm for Pt(bph)$(CO)_2$ in CH_2Cl_2 to 330 nm for Pt(bph)$(CO)_2$ in 4:1 (v/v) C_2H_5OH/CH_3OH to 342 nm for Pt(bph)(dppm) in CH_2Cl_2.

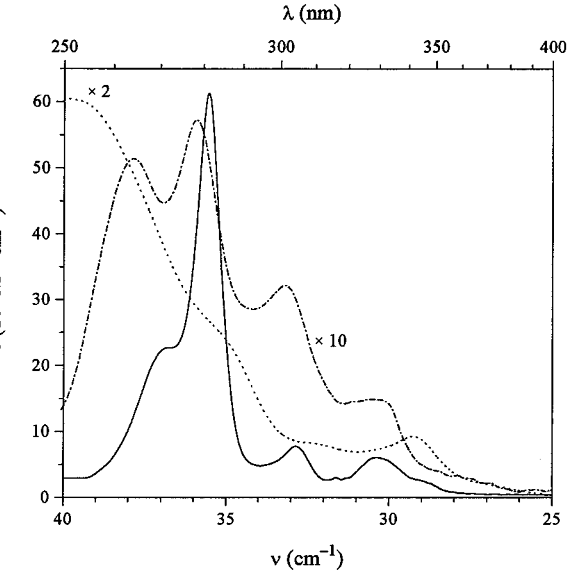

Figure 1. UV−vis absorption spectra of Pt(bph)$(CO)_2$: (—) in CH_2Cl_2 (330 nm, (5.91 ± 0.07) × 10^3 M^{-1} cm^{-1}; 304 nm, (1.04 ± 0.04) × 10^4 M^{-1} cm^{-1}; 281 nm, (4.46 ± 0.06) × 10^4 M^{-1} cm^{-1}); (− • −) in 4:1 (v/v) C_2H_5OH/CH_3OH (330 nm, (1.46 ± 0.22) × 10^3 M^{-1} cm^{-1}; 301 nm, (3.22 ± 0.24) × 10^3 M^{-1} cm^{-1}; 278 nm, (5.73 ± 0.24) × 103 M^{-1} cm^{-1}; 264 nm, (5.15 ± 0.25) × 10^3 M^{-1} cm^{-1}). UV−vis absorption spectra of Pt(bph)(dppm): (•••) in 4:1 (v/v) C_2H_5OH/CH_3OH (342 nm, (5.46 ± 0.15) × 10^3 M^{-1} cm^{-1}) at 296 K.

Room-Temperature Emission Spectra. Emission spectra for Pt(bph)$(CO)_2$ in CH_2Cl_2, 4:1 (v/v) 2-MeTHF/CH_2Cl_2, and 4:1 (v/v) C_2H_5OH/CH_3OH obtained at 296 K are shown in Figure 2 and compared to Pt(bph)(dppm) in 4:1 (v/v) C_2H_5OH/CH_3OH. When excited at 330 nm, the complexes display structured emission, but the high-energy component in CH_2Cl_2 lacks the intensity found in the other solvents and is red-shifted from 506 nm in 4:1 (v/v) C_2H_5OH/CH_3OH to 515 nm in CH_2Cl_2, a decrease in energy of 380 cm^{-1}. When Pt(bph)$(CO)_2$ is excited at 400 nm, the tail of the MLCT absorption band, the emission spectra in 4:1 (v/v) 2-MeTHF/CH_2Cl_2 and 4:1 (v/v) C_2H_5OH/CH_3OH more clearly display a weak, high-energy emission component, whereas in CH_2Cl_2 the high-energy component diminishes in intensity. Properties are summarized in Table 1.

Emission Spectra at 77 K. Emission spectra for Pt(bph)$(CO)_2$ in CH_2Cl_2, 4:1 (v/v) 2-MeTHF/CH_2Cl_2, and 4:1 (v/v) C_2H_5OH/CH_3OH obtained at 77 K are shown in Figure 3A and compared to the one for Pt(bph)(dppm) in 4:1 (v/v) C_2H_5OH/CH_3OH. Excitation at different energies resulted in different

---

(21) Demas, J. N.; Crosby, G. A. *J. Phys. Chem.* **1971**, *75*, 991.

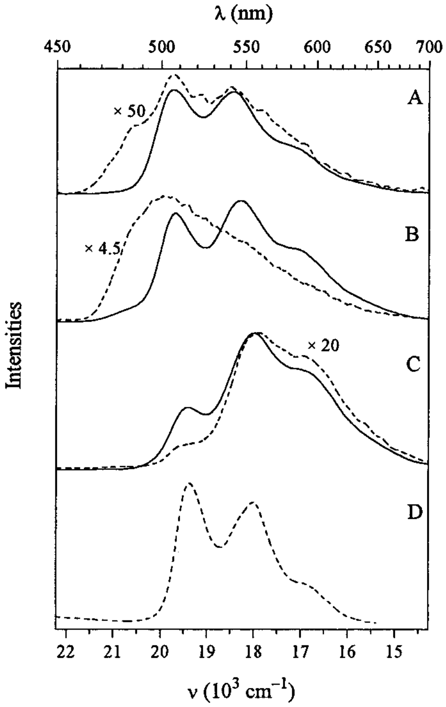

Figure 2. Emission spectra of Pt(bph)$(CO)_2$: (A) in 4:1 (v/v) C_2H_5-OH/CH_3OH (—, excited at 330 nm; ---, excited at 400 nm; (B) in 4:1 (v/v) 2-MeTHF/CH_2Cl_2 (—, excited at 330 nm; ---, excited at 400 nm); (C) in CH_2Cl_2 (—, excited at 330 nm; ---, excited at 400 nm). Emission spectra of Pt(bph)(dppm): (D) in CH_2Cl_2, excited at 330 nm at 296 K.

emission spectra for Pt(bph)$(CO)_2$ but not for Pt(bph)(dppm). At the two extremes, excitation at 330 nm resulted in a structured emission similar to the one for Pt(bph)(dppm), but a broad emission in the red located near 750 nm was observed when the 4:1 (v/v) C_2H_5OH/CH_3OH glass was excited at 501 nm. Two other emissions were observed, a structured emission with a high energy emitting component located at 525 nm when the complex was excited in the 4:1 (v/v) C_2H_5OH/CH_3OH glass at 393 nm and a broad emission located near 660 nm when Pt(bph)$(CO)_2$ was excited in the 4:1 (v/v) C_2H_5OH/CH_3OH glass at 436 nm. While the exact locations of the emission energy maxima differ, similar observations for the complex in a 4:1 (v/v) 2-MeTHF/CH_2Cl_2 glass also occur.

The concentration dependence of the emission components was examined, and the results are shown in Figure 3b for Pt(bph)$(CO)_2$ in the 4:1 (v/v) 2-MeTHF/CH_2Cl_2 and 4:1 (v/v) C_2H_5OH/CH_3OH glasses. As the solution became more dilute, the low-energy emissions vanished and the only one remaining was the high-energy one. Properties are summarized in Table 1.

Excitation Spectra. Excitation spectra for Pt(bph)$(CO)_2$ in CH_2Cl_2, 4:1 (v/v) 2-MeTHF/CH_2Cl_2, and 4:1 (v/v) C_2H_5OH/CH_3OH obtained at 298 K are shown in Figure 4. In CH_2Cl_2 the excitation spectrum corresponds closely to the absorption spectrum, but in 4:1 (v/v) 2-MeTHF/CH_2Cl_2 and 4:1 (v/v) C_2H_5-OH/CH_3OH the excitation spectra exhibit maxima at the low-energy MLCT absorption band. In 4:1 (v/v) C_2H_5OH/CH_3OH and 4:1 (v/v) 2-MeTHF/CH_2Cl_2 at 77 K, the source of excitation for emission located near 650 nm is an excitation band centered at about 433 nm. Under similar conditions but observing emission at 538 nm, similar excitation energy profiles as found at room temperature were observed, but the intensities were nearly 2 orders of magnitude greater.

Emission and Excitation Spectra of Solid Pt(bph)$(CO)_2$. The emission and excitation spectra of solid Pt(bph)$(CO)_2$ are displayed in Figure 5 and compared to the emission and excitation spectrum of Pt(bph)(dppm). Pt(bph)(dppm) displayed the normal structured ^{3}LC-centered emission located at 522 nm, and its excitation spectrum is related to direct population of the triplet emitting state from the ground state. At room temperature, solid Pt(bph)$(CO)_2$, on the other hand, gave a broad emission located at 726 nm and its excitation spectrum commenced with a sharp edge located at 625 nm. A similar excitation spectrum was observed at 77 K, but the emission spectrum contained a major and minor component. The major component was red-shifted from 726 nm at room temperature to 791 nm at 77 K, and its excitation spectrum commenced with the sharp edge at 625 nm and remained fairly linear over the higher energy region. The minor component was located at higher energy (603 nm) than the excitation edge (625 nm) of the major

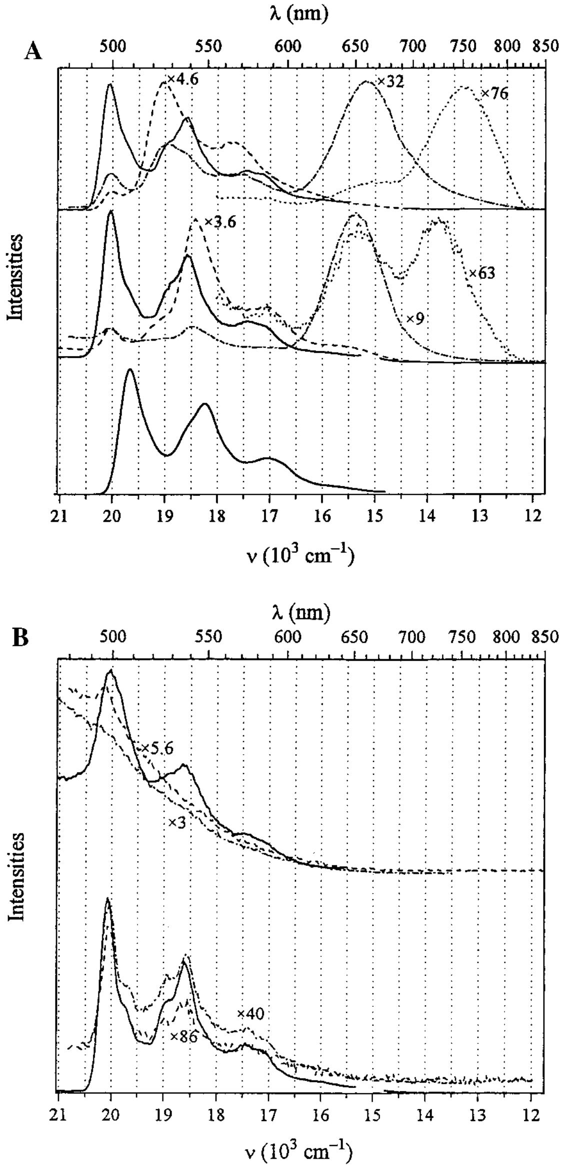

Figure 3. Emission spectra of Pt(bph)$(CO)_2$ as a function of concentration. (A) Concentrated sample: top, in 4:1 (v/v) C_2H_5OH/CH_3OH (—, excited at 330 nm; ---, excited at 393 nm; — • —, excited at 436 nm; •••, excited at 501 nm; middle, in 4:1 (v/v) 2-MeTHF/CH_2Cl_2 (—, excited at 330 nm; ---, excited at 390 nm; — • —, excited at 434 nm; •••, excited at 501 nm. Emission spectra Pt(bph)(dppm): bottom, excited at 330 nm at 77 K. (B) Dilute sample: top, in 4:1 (v/v) 2-MeTHF/CH_2Cl_2 (—, excited at 331 nm; ---, excited at 434 nm; — • —, excited at 390 nm; bottom, in 4:1 (v/v) C_2H_5OH/CH_3OH (—, excited at 331 nm; ---, excited at 436 nm; — • —, excited at 393 at 77 K.

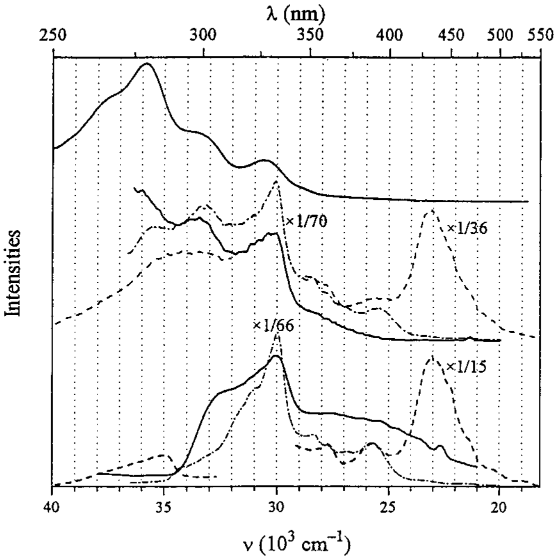

Figure 4. Excitation spectra of Pt(bph)$(CO)_2$ as a function of emission energy and temperature: top, in CH_2Cl_2, detected at 556 nm at 296 K; middle, in 4:1 (v/v) C_2H_5OH/CH_3OH (—, detected at 544 nm at 296 K; ---, detected at 659 nm at 77 K; — • —, detected at 538 nm at 77 K); bottom, in 4:1 (v/v) C_2H_5OH/CH_3OH (—, detected at 544 nm at 296 K; ---, detected at 659 nm at 77 K; — • —, detected at 538 nm at 77 K); bottom, in 4:1 (v/v) 2-MeTHF/CH_2Cl_2 (—, detected at 600 nm at 296 K; ---. detected at 651 nm at 77 K; — • —, detected at 538 nm at 77 K).

component; therefore, its excitation spectrum differed from the one located at 791 nm and displayed two maxima in the 300−400 nm range.

The temperature dependence of the solid emission is shown in Figure 6. As the temperature decreased, the position of the emission maximum decreased in energy and the intensity decreased. The decrease in intensity followed the energy gap law. At 77 K, the emission displayed two energy maxima, one at 745 nm and the other at 791 nm.

Discussion

Absorption Properties of Pt(bph)$(CO)_2$. The electonic absorption spectra of Pt(bph)$(CO)_2$ in solution consist of several prominent peaks along with a number of less prominent features. The low energy bands near 330 and 301 nm show solvent sensitivity and also shift with the nature of the attached ligand. The solvent sensitivity is consistent with an MLCT state assigned as a $d\pi \rightarrow \pi^*$(bph) transition in earlier work,[15,16] and the shift in this transition for Pt(bph)(dppm) compared to Pt(bph)$(CO)_2$ can be related to two different phenomena. First, CO ligands are stronger field ligands than bis(diphenylphosphino)methane lowering the energy of the $d\pi$ orbitals. Second, the CO ligands compete for $d\pi$ electron density with the bph ligand. This also would have the effect of raising the energy of the π^*(bph) level. Thus, both effects would lead to absorption at higher energy for Pt(bph)$(CO)_2$ compared to Pt(bph)(dppm).

The absorptions previoulsy assigned in related systems to $\pi \rightarrow \pi^*$ transitions[15] are solvent dependent. The absorptions broaden, decrease in intensity, and blue-shift in 4:1 C_2H_5OH/CH_3OH compared to CH_2Cl_2. The nature of the hydrogen-bonding solvents, C_2H_5OH and CH_3OH, has a profound effect on the intraligand $\pi \rightarrow \pi^*$ transitions of the bph and CO ligands where the optical transitions become 1 order of magnitude less intense. The exact role of the 4:1 C_2H_5OH/CH_3OH solvent is unclear at this time, but it may be related to the ease of coordination to the open axial sites on Pt(bph)$(CO)_2$ or to distortion of the complex from planarity.

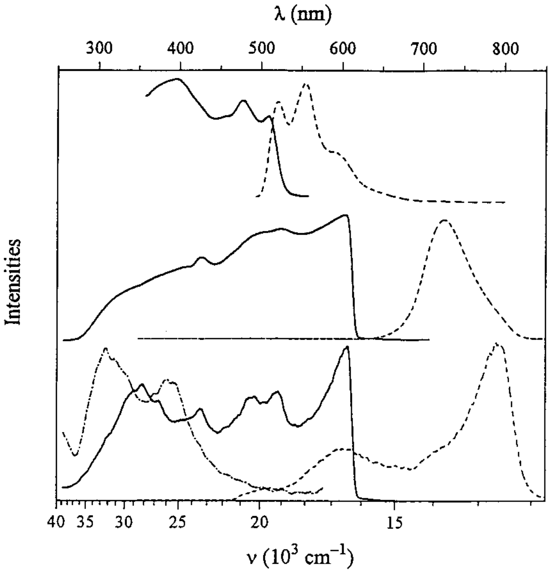

Figure 5. Solid-state excitation and emission spectra of Pt(bph)(dppm): top, at 296 K, — excitation (em. 590 nm) and --- emission (ex. 468 nm). Solid-state excitation and emission spectra of Pt(bph)$(CO)_2$: middle, at 296 K, — excitation (em. 726 nm) and --- emission (ex. 308 nm); bottom, at 77 K, — excitation (em. 791 nm), — • — excitation (em. 603 nm), and --- emission (ex. 308 nm).

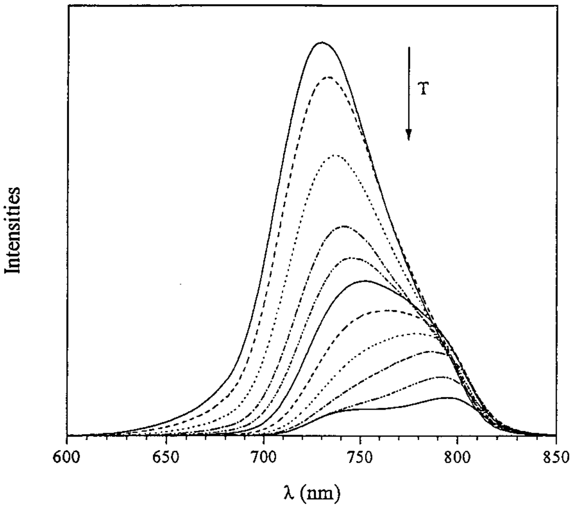

Figure 6. Solid-state emission spectra of Pt(bph)$(CO)_2$ as a function of temperature. From top to bottom: 296, 280, 260, 240, 220, 200, 180, 160, 140, 120, and 100 K.

In the solid state the crystals are green and as previously reported[16] absorb light in the 650 nm region of the spectrum. This absorption can for Pt(bph)$(CO)_2$ be either assigned as a metal centered $d\sigma^* \rightarrow p\sigma$,[22,23] $d\sigma^* \rightarrow p_z(\text{Pt})/\pi^*(\text{CO})$,[24] or $d\sigma^* \rightarrow \pi^*$(diimine)[25−29] transition, depending on the theory followed. The latter assignment is favored since the vibronic structure in

---

(22) Krogmann, K. *Angew. Chem., Int. Ed. Engl.* **1969**, *8*, 35.

(23) Roundhill, R. D.; Gray, H. B.; Che, C.-M. *Acc. Chem. Res.* **1989**, *22*, 55.

(24) (a) Hidvegi, I.; von Ammon, W.; Gliemann, G. *J. Chem. Phys.* **1982**, *76*, 4361. (b) Gliemann, G.; Yersin, H. *Structure and Bonding*; Springer-Verlag: Berlin, 1985; pp 87−153.

(25) Connick, W. B.; Marsh, R. E.; Schaefer, W. P.; Gray, H. B. *Inorg. Chem.* **1997**, *36*, 913.

(26) Houlding, V. H.; Miskowski, V. M. *Coord. Chem. Rev*, **1991**, *111*, 145.

(27) Miskowski, V. M.; Houlding, V. H. *Inorg. Chem.* **1991**, *30*, 4446.

(28) Miskowski, V. M.; Houlding, V. H. *Inorg. Chem.* **1989**, *28*, 1529.

(29) Miskowski, V. M.; Houlding, V. H.; Chi, C.-M.; Wang, Y. *Inorg. Chem.* **1993**, *32*, 2518.

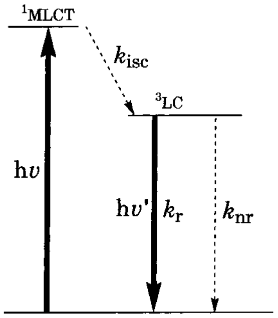

Figure 7. Energy level diagram.

the low-temperature solid-state spectrum is reminiscent of that reported by Miskowski et al.[25-29] and is consistent with vibrational distortion of the bph ligand.

Emission Properties in Fluid Solution. Emission spectra for Pt(bph)$(CO)_2$ at 296 K were similarly structured to those assigned to emission from a ^{3}LC state for the analogues Pt(bph)X_2, X = py and CH_3CN.[15] The emission is attributed to the ^{3}LC state due to the sharp vibrational structure; the dπ orbitals apparently play a minor role. The model shown in Figure 7 is appropiate for explaining the behavior of Pt(bph)$(CO)_2$ in fluid solution which has been verified by directly populating the triplet emitting state from the ground state.[18] Intersystem crossing occurs from a singlet excited state to a triplet ligand-centered state associated with the biphenyl ligand, and then emission occurs to the ground state. However, there are differences in the vibronic progressions for Pt(bph)$(CO)_2$ which vary from 1430, 1400, and 1270 cm^{-1} for samples in CH_2Cl_2, 4:1 (v/v) 2-MeTHF/CH_2Cl_2, and 4:1 (v/v) C_2H_5OH/CH_3OH, respectively. The spectrum of Pt(bph)(dppm) in 4:1 (v/v) C_2H_5OH/CH_3OH displayed vibronic progressions of 1360 cm^{-1}; in CH_2Cl_2 the vibrations were also 1360 cm^{-1}. This vibration for Pt(bph)$(CO)_2$, previously attributed to a ring breathing mode of the biphenyl ligand,[16] clearly is affected by the presence of CH_2Cl_2 or C_2H_5OH/CH_3OH. This effect has only been observed for Pt(bph)$(CO)_2$ and not other Pt(bph)X_2 derivatives. Thus, the structural modification from planarity suggested in the previous section may be the reason for this observation.

The earlier results of directly populating the triplet excited state from the ground state revealed that the intersystem crossing quantum yield from the singlet state to the emitting triplet state was less than one.[18] This result than accounts for the fact that the emission quantum yields varied with excitation wavelength and reached a maximum of 0.084 near 300 nm in CH_2Cl_2. Since this transition is assigned as an intraligand $\pi \rightarrow \pi^*$ transition and the emission quantum yield is much greater than 0.036 obtained by populating the MCLT band at 330 nm, it may mean that energy is partitioned between the lower lying triplet and MLCT states.

Emission lifetimes at room temperature varied from 2 to 3 μs in CH_2Cl_2 and 4:1 (v/v) C_2H_5OH/CH_3OH but were less than 1 μs in 4:1 (v/v) 2-MeTHF/CH_2Cl_2 (0.71 μs) and in the solid state (0.84 μs). The fact that the emission quantum yield is less in the solid state can be readily accounted for on the basis of a different relaxation mechanism.

Emission and Excitation Properties in the Solid State. As shown in Figure 5, solid Pt(bph)$(CO)_2$ shows an intense emission band at 726 nm and an excitation edge at 625 nm. The large shift of the emission maximum from fluid solution and the excitation edge can be explained by the properties of solid-state, chain compounds. As reported earlier,[16] Pt(bph)$(CO)_2$ packs in a columnar structure with Pt−Pt distances of 3.24 Å. For chain packing in square planer complexes of Pt(II), the discrete orbital levels are replaced by bands as shown in Figure 8. Emission then occurs from decay after population of the upper band from the lower one and excitation occurs at an edge consistent with this model. The model further predicts that a decrease in interatomic distance will produce wider bands and, hence, a smaller band gap between the top of the highest filled band and the bottom of the lowest empty band. The red-shift of the emission maximum from 726 to 791 nm upon decreasing the temperature from 296 to 77 K is consistent with band gap narrowing due to a decrease in the Pt−Pt distance upon cooling. Such decreases in Pt−Pt distances were recently measured by Connick et al.[25] for several linear-chain Pt(II) compounds, and red-shifted emission spectra resulting from a decrease in temperature have also been reported by other workers for Pt(II) complexes.[22-32]

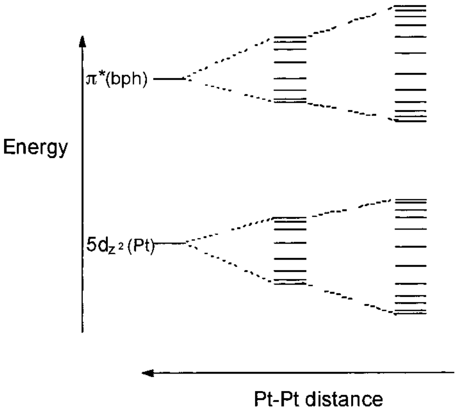

Figure 8. Model for linear chain Pt^{II}(bph)$(CO)_2$.

Three effects are observed from the temperature dependence of the solid-state emission. First, the emission intensity decreases as the temperature decreases which is opposite to the effect normally found in fluid solution. This effect can be attributed to the energy gap law because the energy maxima red-shifted which would have the effect of increasing the nonradiative decay rate and thereby decreasing the intensity.[33] Second, the fact that two energy maxima were observed, one at 745 nm and the other at 791 nm, is suggestive of exciton behavior and the existence of two self-trapped states at 77 K.[24b] Third, a plot of the position of the energy maximum with temperature results in a sigmoidal plot as shown in Figure 9, but the portion of the curve in the temperature range 220−296 K is linear with a temperature coefficient of 3.6 ± 0.1 cm^{-1} K^{-1}. Such variations were studied by Gliemann and Yersin for $Pt(CN)_4^{2-}$, where the changes were approximately linear.[24b] The fact that the plot is sigmoidal may be related to crystal structure packing constraints or a phase transition.

The additional emission decay feature observed in the 77 K spectrum located at 603 nm most likely results from the presence of aggregates of Pt(bph)$(CO)_2$. The excitation spectra of these aggregates, which show broad absorption over the 300−400 nm region, is cleary quite different from the one for the stacked compound at 77 K. Such variations of emission and excitation spectra with the size of particles is now well established[34,35]

---

(30) Thomas, T. W.; Underhill, A. E. *Chem. Soc. Rev.* **1972**, *1*, 99.
(31) Mdleleni, M. M.; Bridgewater, J. S.; Watts, R. J.; Ford, P. C. *Inorg. Chem.* **1995**, *34*, 2334.
(32) Che, C.-M.; He, L.-Y.; Poon, C.-K.; Mak, T. C. W. *Inorg. Chem.* **1989**, *28*, 3081.
(33) Meyer, T. J. *Pure Appl. Chem.* **1986**, *58*, 1193.

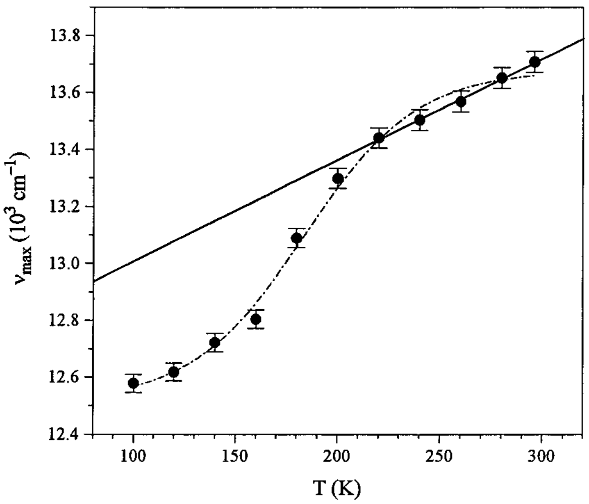

Figure 9. Changes in emission energy at maxima of crystalline Pt(bph)$(CO)_2$ as a function of temperature.

and may be the case here as well. While less likely since the starting material in this study were single crystals of Pt(bph)$(CO)_2$, another possiblity is the 603 nm emission arises from an impurity, such as a CO-bridged species which formed in solution prior to solid formation.

Emission and Excitation Properties in a Glassy Matrix. Emission and excitation properties can be understood, in part, on the basis of the properties observed in fluid solution and in the solid state. Emission at high energy results from decay of the ^{3}LC(bph) state populated by intersystem crossing from singlet states. Emission at low energy occurs from crystallites of Pt(bph)$(CO)_2$ formed upon cooling the matrix from room temperature to 77 K. Emission near 600 nm can be related to the presence of aggregates formed as the solution cools. The remaining emission observed near 550 nm may be due to the presence of dimeric species which emit like exciplex species. The exact nature of this species is unknown, but it may be due to intraligand interactions between metal complexes as reported[9a] for Pt(tpy)Cl$^+$ or formation of bimetallic species. This emission relative to the monometallic species is red shifted as expected.[8]

Emission lifetimes at 77 K in the glassy matrix are approximately 1 order of magnitude larger than in fluid solution at room temperature. The emission lifetime remained fairly constant with the observing wavelength for Pt(bph)$(CO)_2$ in 4:1 (v/v) C_2H_5OH/CH_3OH but did vary systematically with the observing wavelength in 4:1 (v/v) 2-MeTHF/CH_2Cl_2. A plot of ln(k_{nr}) vs E_{em} as shown in Figure 10 resulted in the linear relationship expected on the basis of the energy gap law.[33] The slope of the line was (3.3 ± 0.5) × 10^{-4} cm and the correlation coefficient was 0.98.

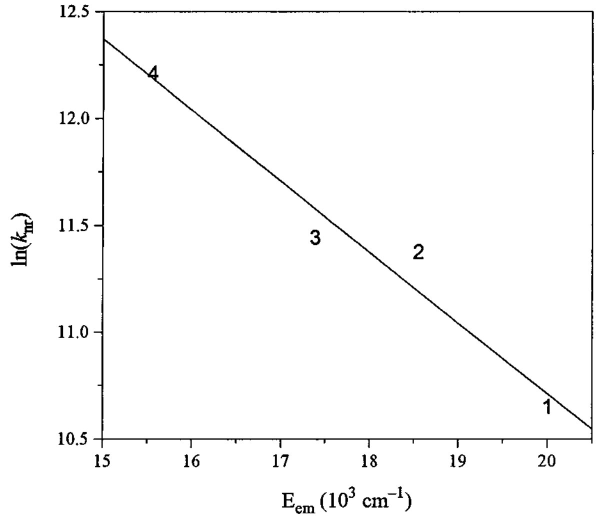

Figure 10. Plot of ln(k_{nr}) vs E_{em} for Pt(bph)$(CO)_2$ in 4:1 (v/v) 2-MeTHF/CH_2Cl_2 at 77 K.

Conclusions

The photophysical behavior of Pt(bph)$(CO)_2$ is complex and can be related, in part, to its crystal structure. The complexes stack alternately in the solid state such that the distance between Pt centers is 3.2 Å.[16] This distance ensures Pt−Pt interactions which leads to semiconductor behavior in the solid state. In solution, these interactions can be broken resulting in monometallic species, but association readily occurs as noted by the presence of several emitting species, except in very dilute solutions. Since the species differ, their excited states also differ such that the monometallic species emit from a triplet ligand-centered state perturbed by the platinum center and the solid material emits from an unfilled band formed by interactions of the metal centers.

Acknowledgment. We thank the Office of Basic Energy Sciences of the Department of Energy for support, the National Science Foundation for the laser lifetime equipment, and Johnson-Matthey for the source platinum compounds.

IC970594F

---

(34) Martin, S. T.; Herrmann, H.; Choi, W.; Hoffmann, M. R. *J. Chem. Soc., Faraday Trans.* **1994**, *90*, 3315.

(35) Choi, W.; Termin, A.; Hoffmann, M. R. *J. Phys. Chem.* **1994**, *98*, 13669.